International Journal of Precision Engineering and Manufacturing (2024) 25:363–381
https://doi.org/10.1007/s12541-023-00928-y

Online ISSN 2005-4602
Print ISSN 2234-7593

REGULAR PAPER

Investigation of the Performance of a V-shaped Inner Plate Array Armor System Against 7.62 mm Caliber Bullets

Erdal Camcı[1] · Mehmet Calışkan[2] · İlyas Berkay Tural[3] · Özgecan Ergü[4] · Fehim Findik[5,6]

Received: 27 January 2023 / Revised: 24 October 2023 / Accepted: 25 October 2023 / Published online: 30 November 2023

Abstract

In this study, the impact resistance performance of the steel internal structure, which is fixed with screws between the front and rear plate, has a 90° bent form and is placed to deflect the penetrating bullet, was measured. This article presents the ballistic performance of the designed armor system against 7.62 mm armor-piercing projectiles with a velocity of 630 to 870 ± 10 m/s, coming at an angle of 90° to the front plate. The study was carried out both experimentally and numerically. Experimental results showed that remarkable ballistic results were obtained among the investigated materials examined in 32 mm thick aluminum-steel-aluminum sheet structures. Numerical and experimental results were compared and a significant correlation was found. In addition to the ballistic performance results, the samples were examined for fracture mechanisms by scanning electron microscopy and EDS analysis.

Keywords Ballistic · Armor structure · Impact · Failure analysis · Finite element method · Numerical analysis

1 Outline

Ballistics has been the intelligent discipline of manhood subsequently earliest periods according to the increasing number of terrorist attacks. In terms of ballistics, laminated metallic shields have some benefits above uniform metallic armor [1]. The benefits derived from the collective ownership of discrete component materials make composites a striking proposal in many respects, i.e. exceptional strength and hardness/mass proportion, decent corrosion resistance, etc.

Impact-associated issues have been an important study theme for years, and great struggle has been devoted to substantially understanding and exactly describing the phenomenon that occurs throughout munitions ballistic penetration [2, 3].

Rigid armor structures consist of numerous plates supported by a flexible material for example ballistic aluminum or steel, or an extraordinary-enactment fiber-reinforced composite. The hybrid preparation of sheets permits the armor structure to overthrow the bullet over on impact, as the ceramic sheet blunts and abrades the bullet because of its extraordinary stiffness, and because the ductile/high tensile back plate absorbs the remaining kinetic energy [4]. Various armor choices are previously obtainable; though, apiece has its own restrictions that limit their extensive usage in numerous requests.

Various analytical models have been proposed for ballistics [5–7], but the impact phenomenon is complex, limiting the usage of implicit form analytical solutions. Hence, numerical methods are favored in such problems. Although there are many studies on impact and penetration in the literature, only a limited number of studies on V-shaped structures have been reported. Also, finite element simulations

✉ Mehmet Calışkan
caliskan@subu.edu.tr

[1] Graduate Education Institute, Sakarya University of Applied Sciences, Serdivan, Sakarya, Turkey

[2] Mechanical Engineering Department, Sakarya University of Applied Sciences, Serdivan, Sakarya, Turkey

[3] Ballistic Protection Tests Unit/Simulation Tests Directorate/Product Verification Directorate, Otokar Automotive and Defense Industry, Atatürk Caddesi, No: 6, 54580 Arifiye, Sakarya, Turkey

[4] Izmir Logistical Department, Ministry of Defence of Turkish Republic, Izmir, Turkey

[5] Metallurgical and Materials Engineering Department, Sakarya University of Applied Sciences, Serdivan, Sakarya, Turkey

[6] BIOENAMS R&D Group, Sakarya University, Sakarya, Turkey

involving material and geometric variabilities along with cutoffs in period are not easy to handle [8].

Today, metallic, and non-metallic materials are utilized as armor. Metallic materials (steel, Al, and Ti-alloys) are used as armor as they have high strength, good toughness, easy shape and weldability, and decent ballistic enactment. However, the density of steel is about 3 times higher than aluminum metal. Therefore, the weight of the steel armor can be reduced by either increasing the angle of attack or increasing the material strength [9, 10]. The strength of materials can be increased in various ways. However, using plated structures is a different and attractive form of design due to decreasing the ballistic limit.

The selection of armor materials is very important in terms of ensuring security in defense applications. Steel is still an important aspirant substance for armor requests because of its good mechanical possessions. It can also be produced easily and is cheaper. However, the chief drawback of steel is its high density. In addition, elevated-strength aluminum alloys also have the possible to be utilized as armor because of their high specific strength.

A group of hybrid composites consisting of metal sheets bonded to a fiber-reinforced polymer substrate is called Polymer Metal Laminate (PML). The metal matrix used for reinforcement may be Al, Mg or Ti and glass, carbon, or Kevlar. The PML system was recognized as a substance with outstanding impact possessions and fatigue resistance, small mass, and adequate corrosion resistance [11].

However, in PML materials, inter-plate stresses cause delamination which causes matrix cracking and fiber damage due to low strength.

Earlier investigations have concentrated on armor plate with a ceramic front sheet and a metallic back sheet [12, 13]. Also, with the initiation of ultra- high molecular weight polyethylene fibers, the interest in ballistic implementation of composite armors made from these fibers has increased. Although a lot of investigation has been completed on the ballistic enactment of high-strength fiber-ceramic shields, there are limited studies on the arrangement of plating the metals, and -high-strength composite laminate [14].

A study made by Ogorkiewicz [15] shows that, 7039 Al-alloy performed improved ballistics than Weldox-armor steels against armor-piercing (AP) bullets. Consequently, consistent with this investigation [15], using 7039 aluminum alloy would be advantageous in terms of weight savings compared to armor steel with the penalty of increasing thickness. In additional previous study, a benchmark for the assortment of metallic armor substances was suggested [16]. In the current investigation, the physical and mechanical possessions of various steels (SAE4130, Hadfield), aluminum and titanium alloys (AA5083, AA7039, Ti–8Al–1Mo–1V) were compared. Consistent with this study, Ti-alloys and Hadfield steel seem to be more beneficial in comparison to the other steel (SAE4130) and Al-alloys (AA5083, AA7039) in terms of ballistic performance. The influence of steel properties on the low-speed impact performance of steel armors was reported [17]. It has been understood that the most perilous feature impacting ballistic performance is target resistance. A review on the ballistic enactment of sheets of single and multi-Plate ductile steel (ranging from 4.7 to 25 mm thickness), rolled homogeneous armor (RHA) (ranging from 8 to 20 mm thickness) and aluminum (for widths in the variety of 6.1 mm) was reported [18] against 6.2 mm bullets in the 800–880 m/s velocity range. They decided that the ballistic resistance of the materials occasionally reduces when the number of Plates is more than two.

Composite armors made with ceramic impact front and great-strength fiber-reinforced composites have been extensively investigated as light armors. Various ceramic substances are characteristically utilized as impact front plates in armor structures for example aluminum oxide (Al2O3), silicon carbide (SiC), boron carbide (B4C), silicon nitride (Si3N4) [19, 20]. These ceramics are supported with high tensile strength rear plates of aramid or polyethylene fiber composites to engross the kinetic energy of the ammunition. While some of these groupings achieve to some degree, the components are costly.

Composite metal foam (CMF) is a hollow and low mass, reasonable strength metal foam entrenched in a metal matrix. This substance showed quite good mechanical possessions [21–23]. The properties of low density and reasonable strength make composite metal foams robust aspirants for armor requests.

In the other work, an attempt was made to discover several substance groupings to adapt the light armor plate structure for 7.62 armor-piercing ammunition and to investigate the associated destruction and distortion behaviors of materials exposed to ballistic influence. In this work, the 30^{o} angle of attack was used to partially take benefit of the angle consequence deprived of creation the angle too unfeasible [24].

In another study, the ballistic behavior of 7075 and 5083 aluminum alloys and HSLA steel, AISI 4140, versus 7.62 mm armor-piercing bullet was investigated. Experimental outcomes displayed that the best ballistic performance among the investigated materials was obtained in 7075-T651 alloy, which maintains ballistic protection with an area density of $\geqslant 85$ kg/m^2 [25].

In an article, the behavior of Weldox 460 E steel plates affected by blunt-nosed cylindrical bullets in the low ammunition velocity regime is investigated. Fast camera was used in experimental studies and finite element code LS-DYNA was applied in simulation studies. The recommended model was applied in simulations of the plate penetration issue and the outcomes were contrasted with the test data [26].

Again, a finite element method was utilized to pretend the ballistic effect and estimate the energy engrossed by the composite metal foam stratum inside the composite armor structure. A 3D model of the composite armor was investigated utilizing a Lagrange creation in Abaqus 16.3 software [27]. Rifled Barrel has 7.62 mm bullet diameter [51 mm long FM (Full Metal Jacket)], and PB (Pointed Bullet), SC (Soft Core Lead), In this study, the response of steel profiles bent in a V-shape (2 mm, 3 mm and 4 mm thick) in aluminum sheets (Fig. 2) subjected to impact loads at various velocities was investigated according to EN 1522 [28].

In his study, İbiş M. investigated the damage mechanisms and ballistic performances of solid, three-layer and nine-layer structures made of hardened AISI 4340 steels experimentally and using the finite element method [29]. The effect of dry contact and adhesive bonded layers on the ballistic performance was also evaluated. It was not possible to reach higher layers with constant thickness with 4340 steels. Higher layer structures were fabricated with Ck75 aqueous spring steel and three-, 20- and 40-layer cases were investigated experimentally. Experiments were carried out with 7.62 mm × 51 (M61) armor-piercing projectile. Perpendicular shots were made to the target surfaces with the experimental setup used.

Although it is a relatively different design field, a study supporting the view that systems with a deflector internal structure similar to the one in this study increases impact resistance was carried out by Jun Hak Lee and his colleagues [30].

A study supporting the importance of impact analysis using the finite element method in the field of mechanical engineering design was carried out by Kwangtae Ha and Jun-Bae Kim [31].

According to the data obtained because of the research, it has been seen that the ballistic strength of monolithic structures made of 4340 steel is superior to the three- and nine-layer structures. The reason for this is the decrease in bending resistance with the increase in the number of layers. While the monolithic structures were damaged by ductile hole formation, concave damage occurred because of bending in layered structures. It has been observed that joining the layers with adhesive increases the bending resistance of the structure and reduces the amount of deformation.

A highly efficient, lightweight composite armor system was produced by using boron carbide ceramics as the impact surface, powder metallurgy processed composite metal foam as the lead kinetic energy absorbing inter Plate, and aluminum 7075 or Kevlar™ panels as the rear plate. The outcomes displayed that the composite metal foams effectively absorbed about 60–70% of the bullet's total kinetic energy and stopped both bullet kinds with less penetration depth and rear plate deformation than specified in the NIJ 0101.06 standard guidelines.

Many substances for example aluminum and steel were utilized to protect the targets and their ballistics tests were carried out. However, ballistic experiments with V-shaped design changes were rarely encountered. Therefore, in this study, the materials used were designed differently, various thicknesses were used, and the conditions providing the best performance were determined by using ballistic experiments using different speeds.

The foremost aims of this study are as follows:

(a) To obtain a successful armor system with cheap and available materials.
(b) To save time in future designs by developing an armor system.
(c) To offer an option in structures that need to be protected by considering the areal density advantage.
(d) To understand better the ballistic performance of V-shaped bent laminated sheets.
(e) To investigate the impact loading of V-shaped steel laminated structures using different material thickness and various shot fire speeds.
(f) To produce an armor for soft targets who is on duty at guardhouse or social anarchy.
(g) Research on V-bend deflector structures mounted between two metals is very limited. Therefore, this research will contribute to the literature.

2 Materials and Design

In Fig. 1, a drawing of the alternative armor system designed for lightening and cheapening in this study is shown. Table 1 shows the dimensions and values of the elements of this structure for different samples. The total mass of the sample 1 version of the designed system is 7.235 kg. The mass of a fully filled block armor of the same dimensions is 20,959 kg. In this case, 1/3 mass reduction is achieved.

St37 steel plates with a thickness of 2 mm and a surface area of 215 × 300 mm were cut by laser. Equal spacing 8 mm diameter holes were drilled on the short side. Three 0.8 mm thick aluminum plates were placed in front of the front plates for display purposes. These aluminums are Al 6000 series materials. The middle structure is twisted both to reduce the areal density and to break up and stop the bullet by traveling a longer distance in the material. 3 mm thick, 215 × 40 mm slices were bent at a 90° angle along the 215 mm long side. Finally, a 4 mm St37 plate was placed at the back as a support plate. The cut of this plate is like the front plates. All these elements were combined with M7 bolts and nuts through the holes and became a whole.

In Table 1, specifications about of designed armor system's samples prepared for experiments have been presented.

The compositions of used metal materials are shown in Table 2. Wholly gunshots were fired at 90 degrees to the target plates at 10 m distance. The effect of projectile speed, plate thickness and ballistic efficiency development techniques were investigated experimentally and numerically. After impact, the depth of penetration was measured,

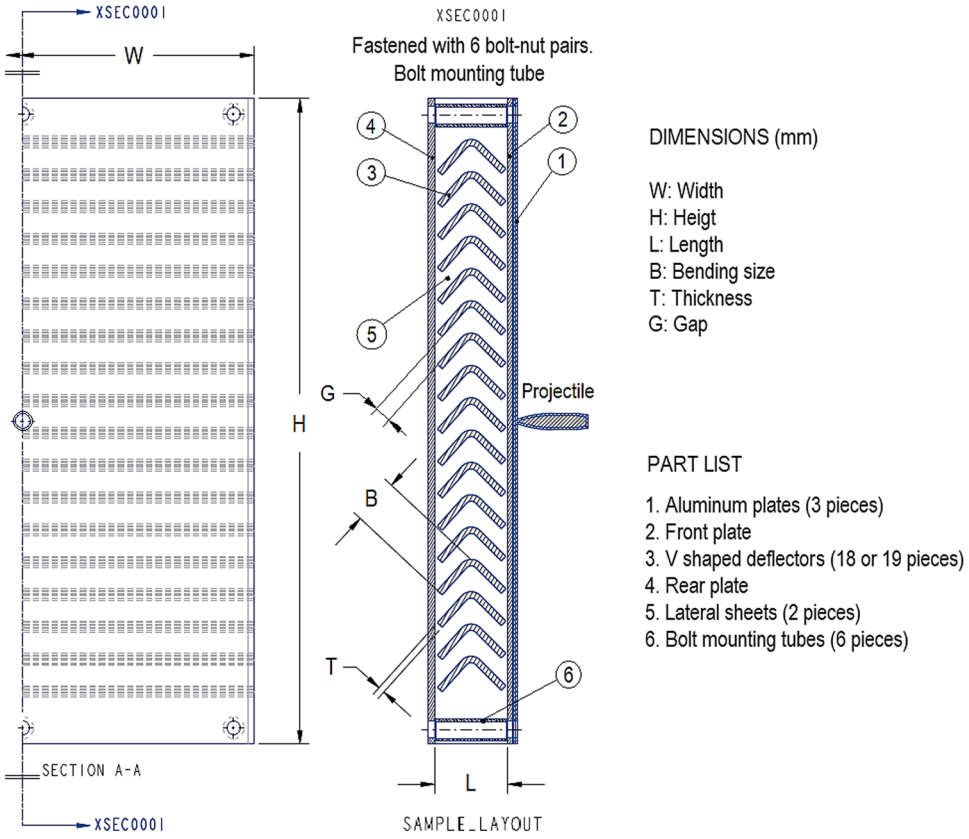

Fig. 1 Symmetrical half drawing of the alternative armor system designed to lighten and cheapen

Table 1 Specifications of the test samples

Sample	System dimensions (mm)											
	W	H	L	B	T	G	1	2	3	4	5	6
1	215	300	32	20	3	15	Al6013, 3 pieces 0.8 mm thick	St37, 2 mm thick	St37, 19 pieces	St37, 4 mm thick	St37, 2 pieces 3 mm thick,	St37, 6 pieces
2			28		1.5		Not available		St37, 18 pieces			
3								St37, 3 mm thick		St37, 3 mm thick		

Table 2 Chemical compositions of used metal plates

Material	Chemical composition
Al 6013 plates	0.6–1% Si, 0–0.5% Fe, 0.6–1.1% Cu, 0.2–0.8% Mn, 0.8–1.2% Mg, 0–0.1% Cr, 0–0.25% Zn, 0–0.1% Ti, Others: (0–0.15%), balance Al
Galvanized steel plate	0.046% C, 0.19% Mn, 0.01% P, 0.011% S, 0.017% Si, 0.041% Al, 0.001% Ti, 0.001% Nb, 0.021% Cr, 0.037% Cu, 0.046% Ni, 40(ppm) N
St 37 steel plate	0.11% C, 0.015% Si, 0.429% Mn, 0.012% P, 0.0064% S, 0.032% Al, 0.005% Cu, 0.004% Ni, 0.021% Cr, 0.000% Mo, 0.001% V, 0.0001 Nb, 0.0018% N, 0.001Sn, 0.000% Ti, 0.0016% B

Table 3 Mechanical properties of used metal plates

Metal plates	Ultimate strength (MPa)	Elongation % min	Hardness HV	Fracture toughness (MPa m^0.5)
Galvanized steel	510	35	140	56
St 37 steel	510	18	143	56
Al 6013 -T6	378	9	150	40

counting plate bending in front of the target plate and protruding behind. The bullets were stopped with aluminum as the front and rear plate, and V-shaped steel sheet metals as the middle structure. Numerical models were analyzed on varying bullet velocities (634 to 868 m/s). The deformation modes that occur in the plate and bullet because of impact loads are good harmonized with the trial consequences. In the numerical analysis, the properties of the boundary circumstances on the resolution were similarly examined.

2.1 Mechanical Properties

Table 3 provides some significant mechanical properties for different sample collections. Hardness levels and strengths for galvanized steel and St 37 steel gave similar values because their carbon ratios were close to each other. The hardness of these steels was measured between 140 and 143 HV (Fig. 2).

3 Experimental Procedure

Experimental procedure executed according to EN 1522 Chart-1 FB-6. 7.62 mm bullets by MKEK (Mechanical and Chemical Industry Corporation) were used in the experiments. Alloy plates of Al-6013 (A6T02PMG-T4) were obtained from Toyota Motor Manufacturing (Turkey). Galvanized steel and St37 steel are standard alloys purchased from the Steel Industrial Products Limited, Turkey. The compositions of the steel and Al-6013 are tabulated in Table 2. The steel sheets were prepared as 300 × 215 mm in 3 different thicknesses (2, 3 and 4 mm). Al-6013 sheets in 300 × 215 mm dimensions and 3 different thicknesses (0.8, 1.6 and 2.4 mm) were processed and used as backing sheets. In metal-to-metal laminated constructions, the front steel sheet and the rear Al-6013 sheet are fastened at the crooks to securely grip the two sheets. The area densities (D) of the incrusted composites were dignified consistent with the formulation below in Eq. 1.

$$D = t_1 d_1 + t_2 d_2 + t_3 d_3 \quad (1)$$

where t_1, t_2 and t_3 are the thickness of Al, steel, and Al, respectively, and d_1, d_2 and d_3 are the density of Al, steel and Al, separate sheets of the incrusted constructions, correspondingly. The test setup is revealed in Fig. 3. All targets were hit at 90 angles of attack with 7.62 mm armor-piercing projectile. Figure 1 denotes an overview of the bullet and essential construction. The projectile has a diameter of 7.62 mm and a real diameter of 6.4 mm. The

Fig. 2 The schematic view of the projectile

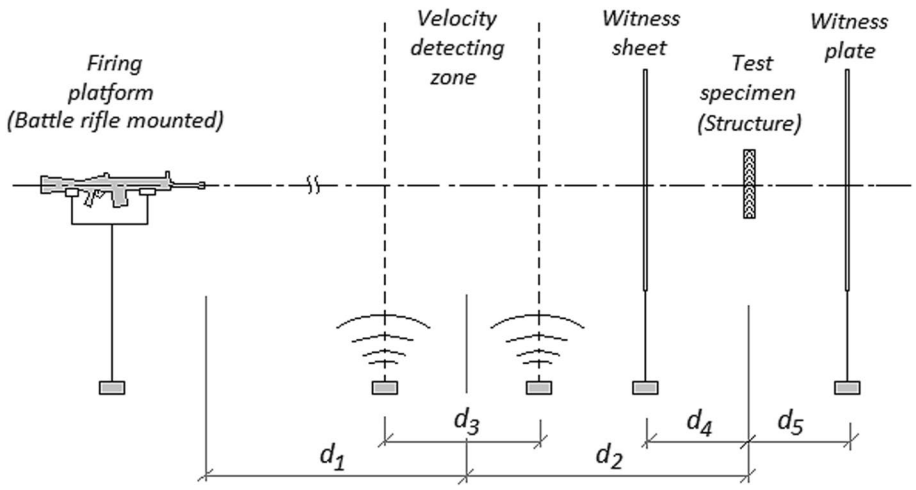

Fig. 3 Representation figure of tentative system. Distances d_1: 7.5 m, d_2: 2.5 m, d_3: 2 m, $d_4 = d_5$: 0.5 m

mass of the bullet is 9.5 g. The hardness of the bullet is 900 VHN. Impact speeds were dignified as 855 ± 15 m/s. The impact speed of the bullet was dignified utilizing infrared light-emitting diode photovoltaic cells by determining the time pause amid intersections caused by the bullet passing along two transverse beams at as table space. The bullet was excited from a space of 10 m. Properly positioning the gun confirmed that the center-to-center space amid any two impact hollows on the sheet was as a minimum three folds the projectile diameter, thereby creating regions of plastic deformation nearby it. The crater is unaffected by the previous ones. For every target sheet was exposed to five gunshots to obtain the ballistic performance. Three distinct samples were verified for apiece sample group. Consequently, more than 50 samples were tried utilizing armor-piercing shells. The most important result in a ballistic test is perforated.

The test was carried out with 7.62 mm × 51 FJ/PB/SC ammunition defined at the FB6 protection level of EN 1522-1523 standard. Ordinary metallographic procedures were utilized for the microstructure. Steel samples were etched using Nital (2%HNO3 + 98% Methyl Alcohol) and Al-6013-T6 specimens Keller's chemical (5 ml HNO3, 3 ml HCl, 2 ml HF and 190 ml water) to disclose the micrograph. The light and electron microscopes were utilized to detect the dissimilar phases existing in the micrograph of the plates. The hardness of metallic specimens was dignified consistent with ASTM E 140-02 utilizing an AFFRI Vickers hardness machine. 30 kg load was utilized for steel specimens and 5 kg load was utilized for Al-6013-T6 specimens to control hardness. In the hardness tests, five quantities were made for every sample. The fracture surfaces of mutually steel and Al-6013-T6 were perceived in a LEO SEM (scanning electron microscope) to identify the fracture mode.

4 Numerical Study

In this research, ANSYS LS-DYNA finite element software, whose competence in ballistic analysis has been proven by many studies in the literature, was used. LS-DYNA is a finite element software used for non-linear analysis of structures subject to large deformation, especially with the small-time interval method. It uses different contact-effect algorithms that allow the analysis of difficult contact problems such as element deletion with ballistic effect. It is necessary to use data cards suitable for analysis for the effective use of this software, which has a wide library of material models and different contact algorithm types. The Lagrangian method used in finite element analysis in this study is based on the partitioning of the continuous material to solve the dynamic stress wave propagation that is already present in ballistic simulations [32].

The rigid body is divided into 'N' elements, and this is called the mesh structure. In Lagrangian calculations, the material is embedded in the mesh. Thus, the displacement, rotation and distortion of the network structure can represent the material behavior. With the increase in the density of the network structure, the accuracy of the calculations increases, and it can cause sharp increases in the solution time. Therefore, the most appropriate mesh structure should be chosen to reach the situations where ignorable deviations are seen in the variation of the results. The most suitable mesh is the one where the deviations in the solutions are negligible and the lowest computation time is obtained. For the damage estimation of the shot plates, the number of elements in the area in contact with the bullet was concentrated, where the dimensions of the element were reduced from 1 to 0.25 mm. (Similar analyzes in the literature indicated that it is adequate to use 0.25 × 0.25 × 0.25 mm 3 elements in the region where the number of elements is dense for metals [33, 34]. In Fig. 4, the finite elements model representing the 1st sample—1st shot experiment is seen. The CAD model is parametric It was modeled in the PTC Creo software. Bonded contact mechanism available in the LS-DYNA finite element program was used to define the assembly structure of the test sample. No gaps are left between the parts and the friction coefficient is ignored. In the simulations, Johnson–Cook constitutive equation and damage model, which has been proven by many studies in the literature, were used in modeling the behavior of metal armors under impact. The Johnson–Cook (JC) strength model is the yield stress equation that has been revealed because of experiments performed at different strain rates and at various temperatures (Eqs. 2 and 3). It can define the stress and strain relations of metal materials under high deformation, high strain rate and high temperature conditions [35].

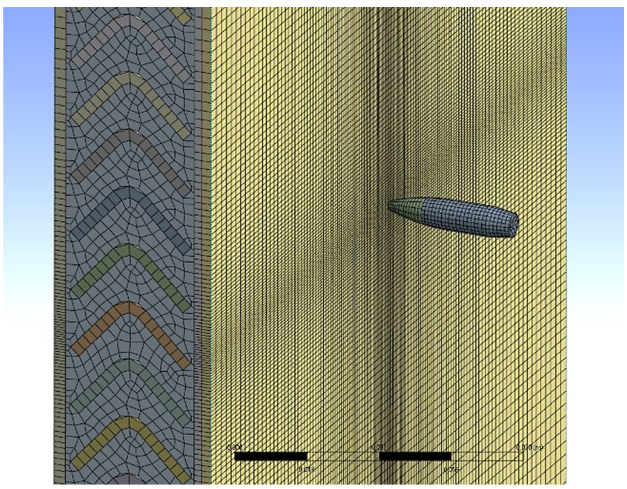

Fig. 4 Finite element model of the sample 1 specimen

$$\sigma_{eq} = (\varepsilon_{\mathrm{eq}}, \dot{\varepsilon}^{*}_{eq}, T) \tag{2}$$

$$\sigma_{eq} = (A + B.\varepsilon^{n}_{eq})(1 + C.\ln \dot{\varepsilon}^{*}_{eq})(1 - T^{*m}) \tag{3}$$

Here, ε_{eq}; Defines the hardening with the material constants *A, B* and $n.\dot{\varepsilon_{eq}}^{*}$; Defines strain hardening with constant *C.T*; Expresses the thermal softening arising from the adiabatic temperature increase with the constant *m*.

The JC model is defined by the mathematical multiplication of the three states mentioned above. The first bracket in the equation considers the increase in yield stress due to hardening. The shear stress required to produce shear in metal always increases with an increase in strain. Hardening occurs because of the interaction of dislocations with barriers that prevent the movement of crystalline structures within the material. The second bracket defines the increase in yield strength with increasing strain rate, $\dot{\varepsilon_0}$ is a dimensionless parameter and is expressed with Eq. 4 [36].

$$\dot{\varepsilon}^{*}_{\mathrm{eq}} = \dot{\varepsilon}_{eq} / \dot{\varepsilon}_0 \tag{4}$$

This temperature-dependent expression reveals the thermal softening of the material due to the thermal-plastic instability. This term evaluates the ratio of the yield stress at elevated temperature to the yield stress at room temperature.

$$T^{*} = (T - T_{\mathrm{r}}) / (T_{\mathrm{m}} - T_{\mathrm{r}}) \tag{5}$$

Here, the "r" subscript denotes the room temperature, and the "m" subindex denotes the melting temperature. It is assumed that the temperature increase occurs adiabatically. The temperature increase due to adiabatic heating is calculated by the following equation.

$$\Delta T = \int_{0}^{\dot{\varepsilon}_{eq}} \chi \frac{\sigma_{eq}.d.\varepsilon_{eq}}{\rho.c_p} \tag{6}$$

Here, ρ is the material density, *Cp* is the specific heat, and *X* is the Taylor–Quinney coefficient, which represents the rate of plastic deformation work converted into heat. It is appropriate to take the Taylor–Quinney coefficient 0.9 for steels [34]. *D* is a function of 5 different damage parameters, the fracture state occurs when $D = 1$.

$$D = \sum \frac{\Delta\varepsilon_{eq}}{\varepsilon_f} \tag{7}$$

Here, $\Delta\varepsilon_{eq}$ denotes the increment of the equivalent plastic unit deformation that occurs during an integration cycle. ε_f is the unit strain for fracture under certain strain rate, temperature, and equivalent stress conditions. In the original Johnson–Cook model, the second parenthesis expressing the sensitivity to the unit strain rate was modified to avoid undesirable effects in the case of $\dot{\varepsilon}_{eq} < 1$.

$$\sigma_{eq} = (A + B\varepsilon^{n}_{eq})(1 + \dot{\varepsilon}^{*}_{eq})^{C}(1 - T^{*m}) \tag{8}$$

In this study, it was considered appropriate to use the modified Johnson–Cook (MJC) material model given in Eq. 7 to observe the damage effects. In addition to Johnson–Cook damage parameters, temperature-based damage has been defined in simulations. The critical temperature value has been taken as $T_{cr} = 0.9T_{\mathrm{m}}$ [36]. This means that if the temperature reaches 90% of the melting point, the elements will be erased. It is assumed that when the critical temperature is reached, the strength of the material drops too much, and it cannot resist impact. Johnson–Cook damage parameters for fracture strain are given in Eq. 9.

$$\varepsilon_f = \left(D_1 + D_2 \exp\left(D_3\sigma^{*}\right)\right)\left(1 + D_4 \ln\left(\dot{\varepsilon}^{*}_{eq}\right)\right)\left(1 + D_5 T^{*}\right) \tag{9}$$

Table 4 Material properties for JC model

Material	Strength parameters				
	A (MPa)	B (MPa)	n	C	m
St 37	200	250	0.36	0.022	1
Al 6013	265	426	0.34	0.015	1
Bullet	1539	477	0.18	0.012	1

Table 5 Material properties for MJC model

Material	Damage parameters				
	D_1	D_2	D_3	D_4	D_5
St 37	0.05	3.44	− 2.12	0.002	0.61
Al 6013	0.05	5	− 3	0.003	0.85
Mermi	0	0	0	0	0

The effects of the three parentheses on the fracture strain can be expressed as the stress triaxiality effect, the strain rate effect, and the temperature effect, respectively. D_1, D_2, D_3, D_4 and D_5 represent the d obtained from the tests and $\sigma^* = \overline{\sigma}/\sigma_{eq}$ stress triaxiality.

The values of the material models used in the model can be seen in Tables 4 and 5.

In Fig. 4 finite element model has been shown. This is a full 3D Ls-Dyna model, the bullet has initial velocity, the lateral sheet metals are fixed, analysis type is explicit. The model includes a total of 90,403 elements and 186,961 nodes, 466 of which are Wedge and 89,937 are Hexahedral. Gravity defined. Contact connections are defined between the parts.

5 Results and Discussion

5.1 Cautious Outcomes

All numerous kinds of specimens with Al back plate, target plate with 32 mm sample thickness considered as the extreme permissible penetration as said by the NIJ 0101.06 standard, were pierced by the projectile at velocities of 868 m/s. However, in the shots fired at 700 m/s and slower speeds, the target was not penetrated in any way.

The images of the damaged bullet cores and the rear surface of the Al-Steel-Al armor panel subsequently the NIJ-Type III impact experiment are exposed in Fig. 4A and B, correspondingly. The V-shaped steel impact plate effectively dulled and eroded bullets upon impact. As perceived in Fig. 4A, a very minor quantity of NIJ-Type III projectile jacket substance is left entrenched in the armor. Outward cracks on the copper sheet appear to propagate from the impact area seen in Fig. 4A, forming an outward crater. The hard steel core successfully spreads the charge onto the copper jacket, which will engross most of the bullet's kinetic energy from side-to-side plastic distortion and consequent concentration. As perceived in Fig. 4B, these remaining tensile stresses behind the aluminum sheet created outward cracks spreading from the impact zone. Some pieces of aluminum were evicted from this region. This surveillance prompted the impression of totaling a tinny back plate sheet after the aluminum to engross these remaining tensile stresses and clasp any low-speed parts (Fig. 5).

In ballistic impacts, utmost of the kinetic energy of the bullet is converted to brittle fracture of the steel beneath tension and compression, plastic distortion of the bullet and back-up sheet. By means of an energy method [37], the energy engrossed by every Plate in the composite armor structure can be approached. Now of impact, the bullet's kinetic energy (EKE), the energy utilized for the plastic distortion of the bullet (E_{bullet}), the energy engrossed by the steel (E_{steel}), the energy engrossed by the aluminum sheet (E_{Al}) are conveyed to the armor structure. The energy engrossed by the back-up plate ($E_{backing}$) is the energy remaining from the target in the case of perforation (E_{res}) given in (Eq. 10):

$$EKE = E_{bullet} + E_{steel} + E_{Al} + E_{backing} + E_{res} \tag{10}$$

Comparable investigations on the energy captivation of armor structures have been described in the earlier works [38]. Energy per unit volume of substance for bullet, steel and Al, Eq. 2 can be considered from the corresponding stress–strain diagram by computing the zone underneath the curve by means of a strain energy (w_p) process. (Eq. 11)

$$W_p = \int \sigma d\varepsilon \tag{11}$$

where W_p is fundamentally the zone beneath the stress–strain diagram in J/m^3. Utilizing the substance possessions of every sheet and increasing the assessment of this strain energy by the overall quantity of substance under distortion (bullet, aluminum, steel, aluminum) per Plate, the entire kinetic energy dissipated by every constituent of the composite armor structure is considered.

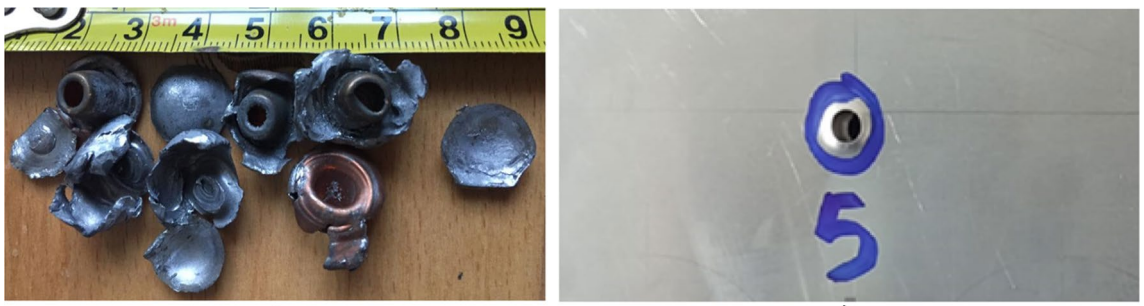

Fig. 5 Digital images of an impact zone on an armor structure deprived of backing sheet: **A** front strike face displaying wide-ranging capture of the gunshot and **B** rear face illustrating swollen of Al-plate and trivial extent of cracking because of tensile stresses

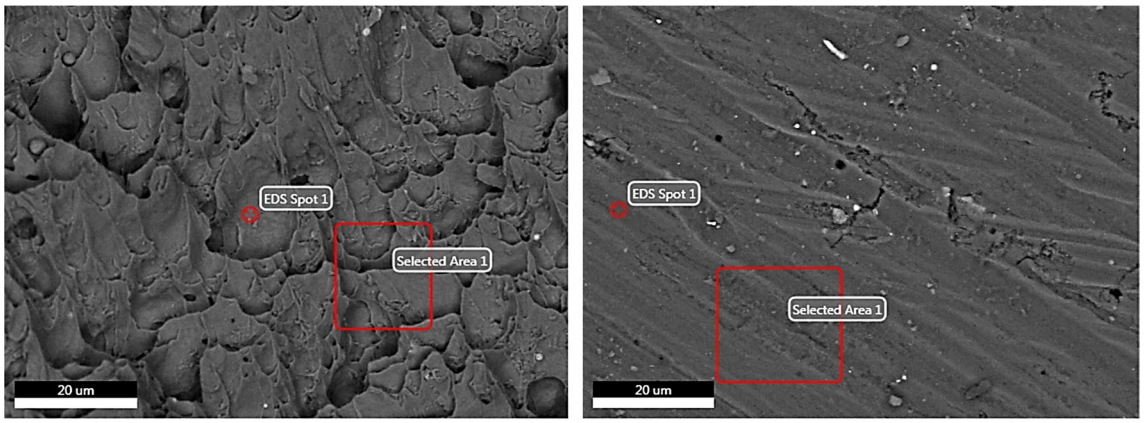

(a) (b)

Fig. 6 **a** Microstructure analysis of St 37 and **b** Al-6013

Within the white-appearing ferrite matrix, the microstructure of the black-colored pearlite fields is visible in both steels (Fig. 6a, b). Instead, the hardness stages were 150, and 128 HV for 6013-T6, and 2024-T3, respectively. The artificial aging process in 7075 alloy reasons the creation of compatible precipitates which lead to great hardness and hence strength in the construction. However, excessive aging degrades the consistency of the precipitates with the matrix atoms causing some decrease in together hardness and strength.

5.2 Ballistic Performance

The factors affecting ballistic performance are briefly as follows: Mechanical properties of armor materials, bullet type, bullet shape and velocity, armor system manufacturing method, material production qualities, test standards, bullet impact angle and position. When the tests performed under these effects are evaluated, the mechanical properties of St37 in the first sample are largely successful. It was not drilled at a speed of 700 m/s and this speed is in the high-speed impact class. Also, the highest pitting and tearing of the back support plate at the actual drilling speed (866 m/s) indicated that the material was ductile and had good ballistic energy absorption. The mid-V deflector caused the structure to blunt the bullet tip and put more pressure on the rear support plate. The high area density of this building necessitated a lighter structure. This lightness is provided in the second and third structures. However, the deflector structure could not fully fulfill the function of fragmenting or deflecting the projectile within the armor system. Because even the fins were punctured and only slightly reduced the velocity of the projectile. Test shells fired perpendicular to the armor systems deviated a little (8–10 degrees) from the firing line.

According to the bullet impact velocities and ballistic performance determination test, their performances were close. Although the total thickness of the front and rear support plates was the same in the third sample, the rear support plate was kept thicker by making the front 2 mm and the rear 4 mm in the second sample. In the third sample, both the front and rear support sheets were made with a thickness of 3 mm. Their ballistic performances are close to each other. Ballistic boundaries, on the other hand, are formed differently.

Penetration of the bullet into any area of the target is called penetration; while perforation happens once the bullet passes from side to side the target [39]. In the further arguments, puncture can be described as full penetration. The ballistic enactment of the examined metallic materials was assessed by seeing the possibility of puncture of these materials from 5 shots specified in Table 6. All the samples numbered 1, 2 and 3 did not cause any perforation to the target when the bullet velocity was below 700 m/s. However, the target is fully perforated in the structure 1 at projectile velocities above 701 m/s (e.g. 868 m/s).

The graphical interpretations of the experiments whose results are given in Table 6 can be seen in Figs. 7, 8 and 9.

Figure 10 shows front and rear views of sample groups 1, 2 and 3 after ballistic testing. Petaling, a collective failure mode for ductile substances underneath ballistic impact, shaped on the reverse side of these samples after projectile ejection. In addition, the ductile hole creation mechanism took place in those samples deprived of any cracks.

Table 6 Ballistics test results

Sample	Impact-velocity (m/s)	Front plate penetrated	Total perforated	Witness foil	Measured front plate deformation (mm)	Measured rear plate deformation (mm)
1	631.45	Yes	No	No	0.9	7.4
	644.98	Yes	No	No	5.0	8.6
	655.35	Yes	No	No	7.1	9.4
	700.23	Yes	No	No	7.3	8.3
	868.84	Yes	Yes	Yes	8.6	22.5
2	586.38	Yes	No	No	6.3	10.7
	678.17	Yes	Yes	Yes	8.8	21.6
	692.55	Yes	Yes	Yes	4.0	26.6
	728.78	Yes	Yes	Yes	3.0	26.1
	768.68	Yes	Yes	Yes	6.3	17.1
3	611.06	Yes	No	No	10.0	12.7
	647.72	Yes	No	No	10.7	13.3
	649.93	Yes	No	No	10.9	14.0
	653.34	Yes	No	No	10.7	13.5
	660.87	Yes	No	No	9.7	14.2
	675.83	Yes	Yes	Yes	10.7	19.4

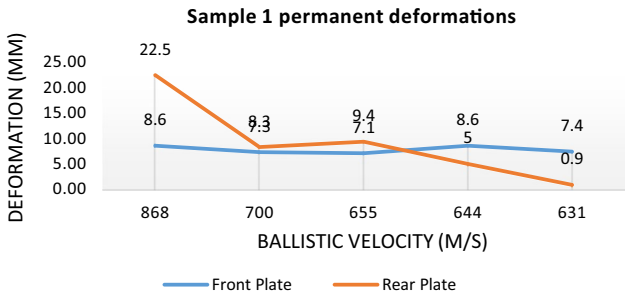

Fig. 7 Plate deformation values

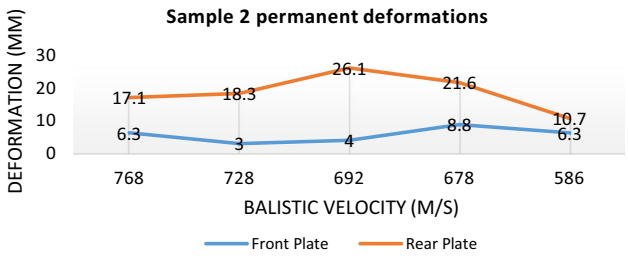

Fig. 8 Plate deformation values

An increment in the hardness of a material causes the bullet to become more difficult to propagate, increasing wear and breakage of the bullet. Fracture mechanisms of ductile

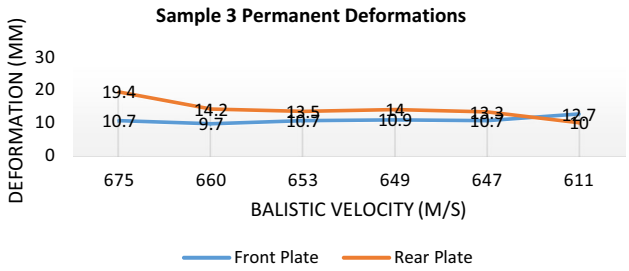

Fig. 9 Plate deformation values

hole creation were perceived in failed samples. For AISI 1006 (St 37) steel, samples with a hardness of 143 HV were pierced by bullets, creating a ductile hole as perceived in 6013-T6 aluminum alloy samples. This result agrees with the previous studies; because in previous studies, ductile fracture was observed in materials with low hardness (38 HRC), and brittle fracture in materials with high hardness (50 HRC) [25].

Figure 11 shows the macro vision of the fracture surface of sample 1 (St37) by SEM. Shear bands can be observed because of reproduced tensile stress waves. The shear bands exposed that the ballistic impact causes cyclic forcing in the sheets because of numerous reproductions of the tensile waves [10]. It can be supposed that most of the failure is because of these tensile stresses. Figure 12 displays the SEM micrographs of the fracture surface of sample 2 near the impact region and in the central region over the thickness of the sample. In the impact area, pits

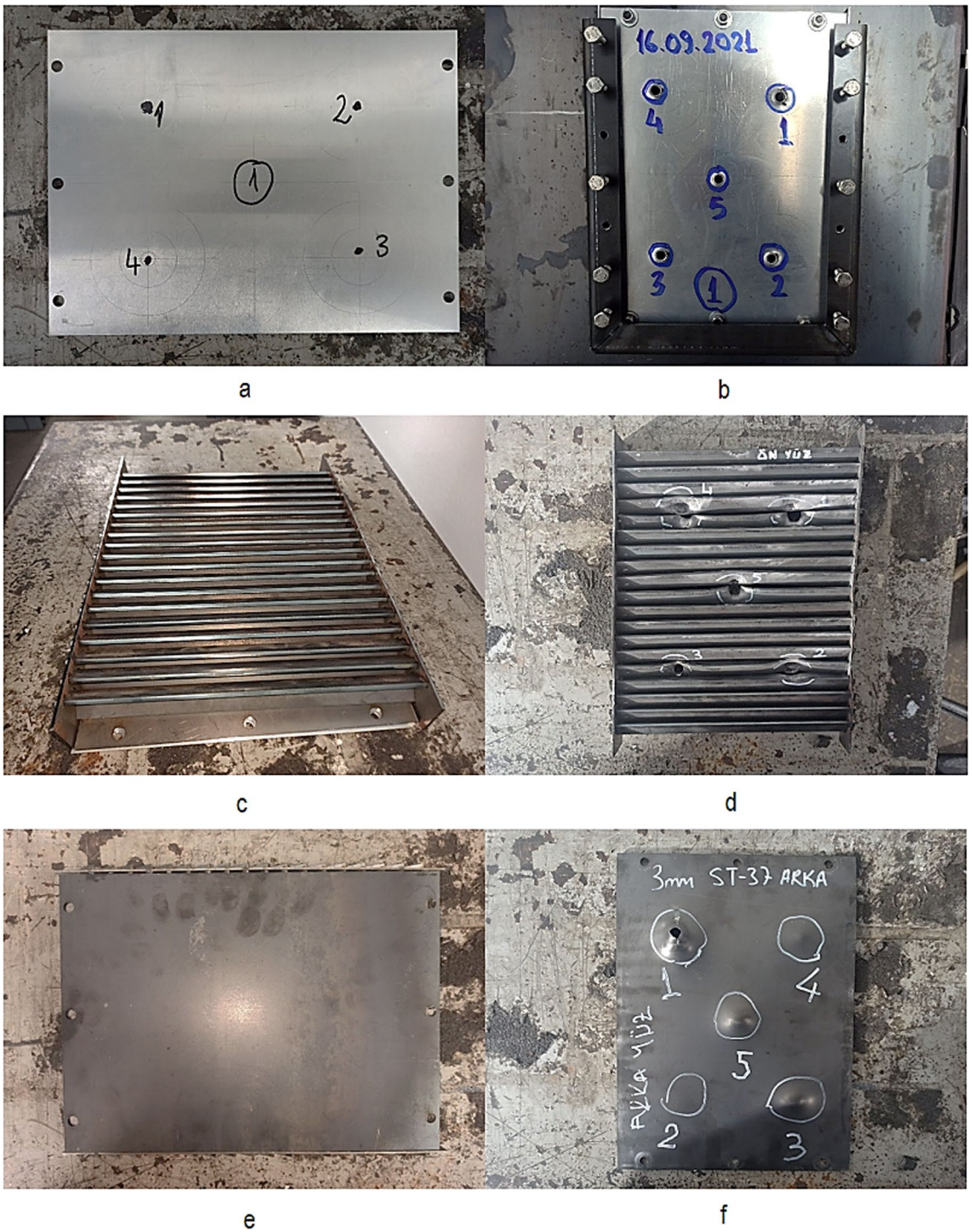

Fig. 10 Armor system (sample 1) parts before and after ballistic testing. (**a**, **b** Front plates (Al6013 + St37), **c**, **d** V shaped deflector sheet-metals, **e**, **f** Rear plate)

were observed at a deepness of about 6 mm from the brink. In the rest of the fractured surface, ductile fracture type was observed throughout the thickness. Furthermore, mainly intergranular type fracture was perceived from the fracture surface of the specimen. Also, confined melting of lead from the bullet occurred in the impact region of the samples.

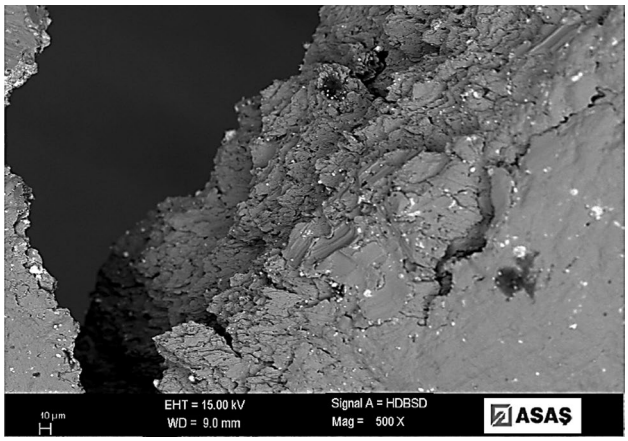

Fig. 11 Macro vision of the fractured surface of the sample 1 (St37) through the thickness

5.3 Numerical Results

Figures 13 and 14 illustrate the simulations in FEM of the front and rear faces on armor system after a ballistic impact at bullet speeds of 868 m/s and 650 m/s, correspondingly. In numerical simulations, analyzed system is sample 1. In the armor system, the bullets have been effectively stopped at 631 m/s impact velocity and lower bullet velocities according to the NIJ 0101.06 standard. Also, it was seen that the armor plates damaged the bullet because of impact. The obtained numerical results are consistent with the current experimental results.

Figures 15 and 16 present the deformation comparisons between experimental and numerical analyses. Considering that it will be useful in evaluating the results of this study, the results of the study given in reference [29] have also been included in this comparison.

When the results in Figs. 15 and 16 are examined, it is seen that there are fluctuations in the experimental results, whereas the numerical results give more stable results. Since the experimental measurements were made by disassembling the armor system after the experiment, some particle ruptures are possible. Therefore, it is thought that this fluctuation may be due to this reason. On the other hand, it is not surprising that the JC numerical material model yielded more stable results. At this stage, researchers are advised to examine the similarity of deformation behavior as well as deformation values. In this study, it was observed that perforation and penetration behaviors were similar at ballistic upper and lower limit velocities. It is gratifying that this consistency exists. In addition, it is thought that the reason for the inverse proportionality of the bullet velocity and the deformation amounts is the adiabatic shear assumed to be in terminal ballistics.

In addition, it is emphasized in Figs. 15 and 16 that the results obtained in the 3-layer armor system trials in reference [29] overlap with the results obtained in this study. These results show that this alternative armor system, which is designed to be less expensive and low-density compared to monolithic armor plates, can be used successfully (Figs. 17, 18, 19, 20).

6 Conclusions

The assortment of appropriate armor supplies for defense claims is significant in terms of security. Steel is an important nominee material for armor requests because of its loftier mechanical properties, manufacturability, and inexpensiveness. Alternatively, the chief drawback of steel is its comparatively high density. Subsequently steel and

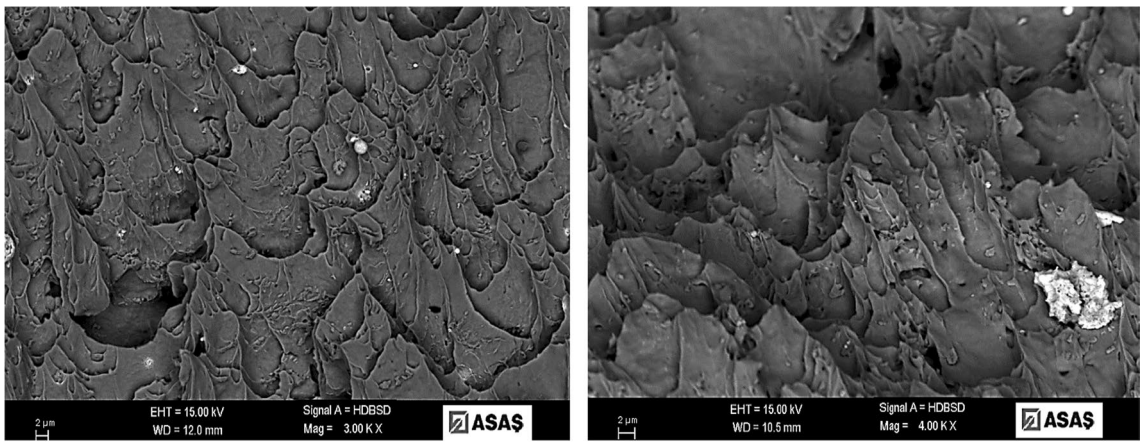

(a) (b)

Fig. 12 SEM micrographs of fractured surface of sample 1 (St37) **a** close to the impact region and **b** at the central area over width

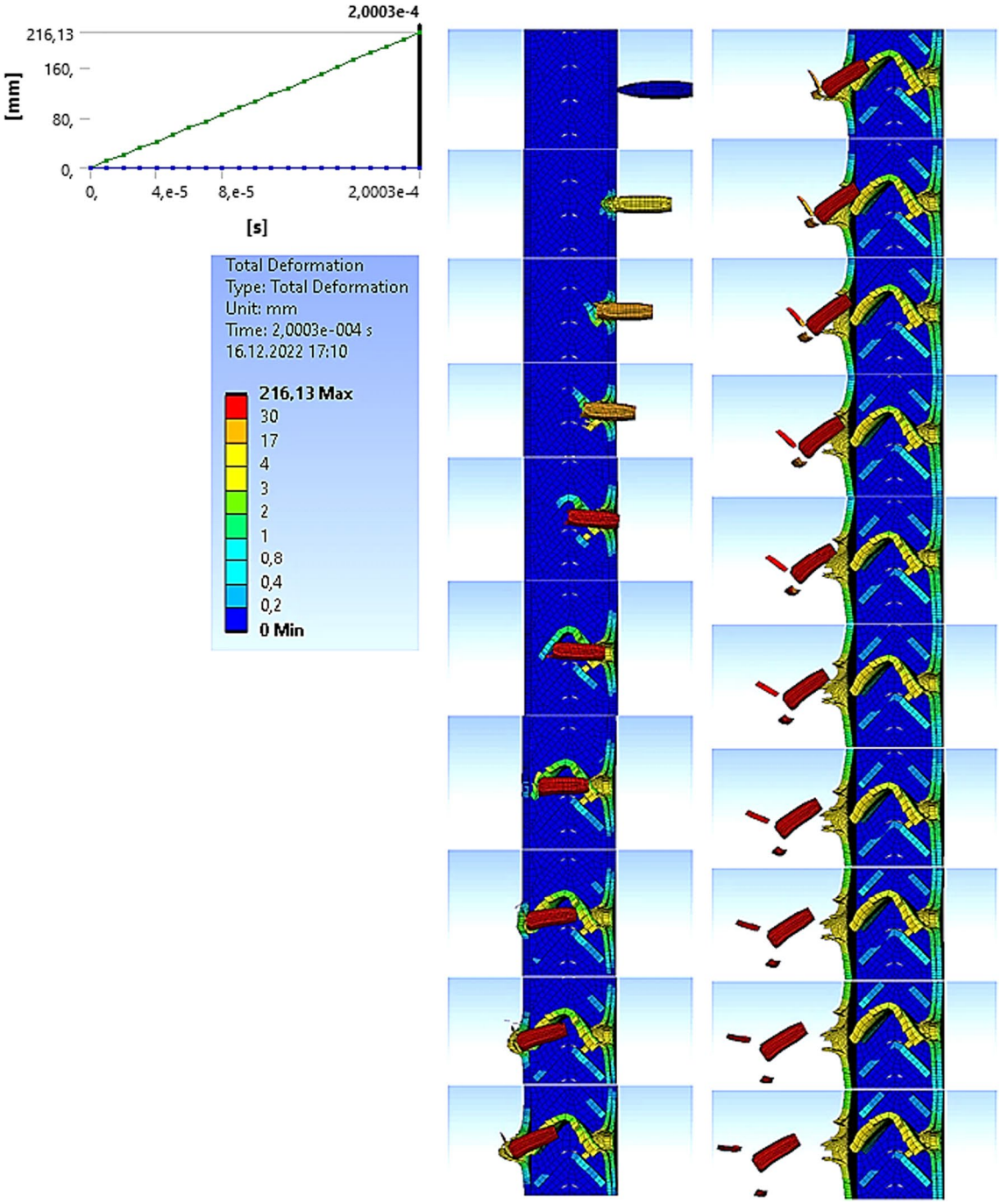

Fig. 13 Deformation results of the simulation made with ballistic upper limit velocity (868 m/s)

high-strength aluminum alloys can possibly be utilized as armor because of their comparatively greater specific strength. In this study, ballistic investigations of the armor material containing plated material consisting of Aluminum and Steel were carried out. The results obtained are summarized below:

- The gap between the target sheet frame and the firing structure was 10 m. The target was fully fired at an angle of 90 degrees to the plates. The bullets were stopped by Plates of lightweight aluminum as the front and rear plate and specially designed V-shaped steel Plates as the middle Plate.

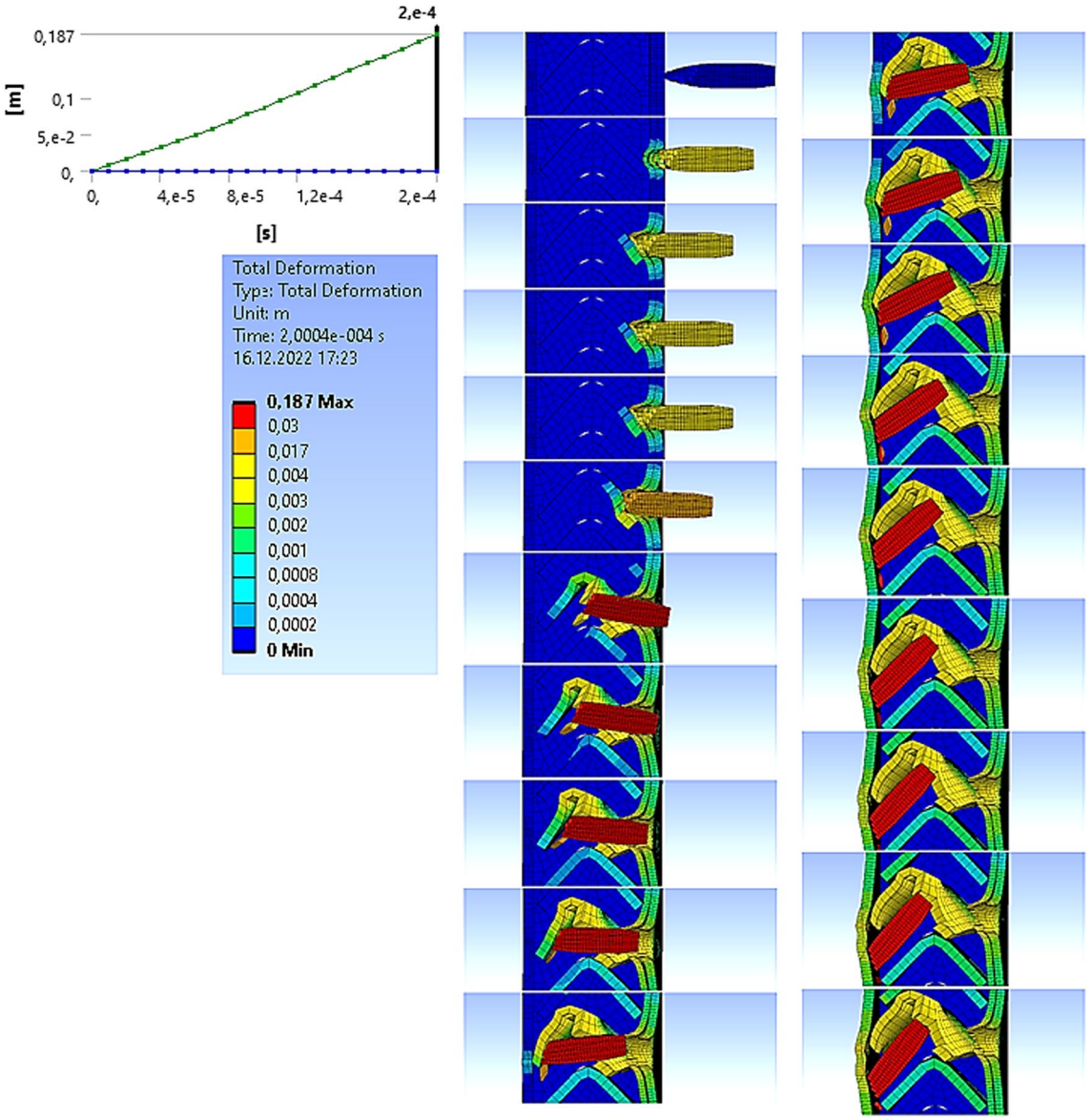

Fig. 14 Deformation results of the simulation made with ballistic lower limit velocity (631 m/s)

- 7.62 mm bullets belonging to MKEK (Mechanic and Chemical Industry Inc.) company were used in the experiments. Steel plates were cut in a V-shape with dimensions of 300 × 215 mm and in 3 different thicknesses (2, 3 and 4 mm). Al-6013 sheets with the dimensions of 300 × 215 mm and 3 different thicknesses (0.8, 1.6 and 2.4 mm) were processed and used as the backing sheet.
- All various samples with Al back-plate, target plate with 32 mm sample thickness reflected the utmost permissible penetration consistent with the NIJ 0101.06 standard, were pierced by the projectile at velocities of 867 m/s. However, the target was not penetrated in any way in the shots fired at 700 m/s and lower speeds.
- Hardness levels and strengths for galvanized steel and St 37 steel gave similar values because their carbon ratios were close to each other. The hardness of these steels was measured between 140 and 143 HV.

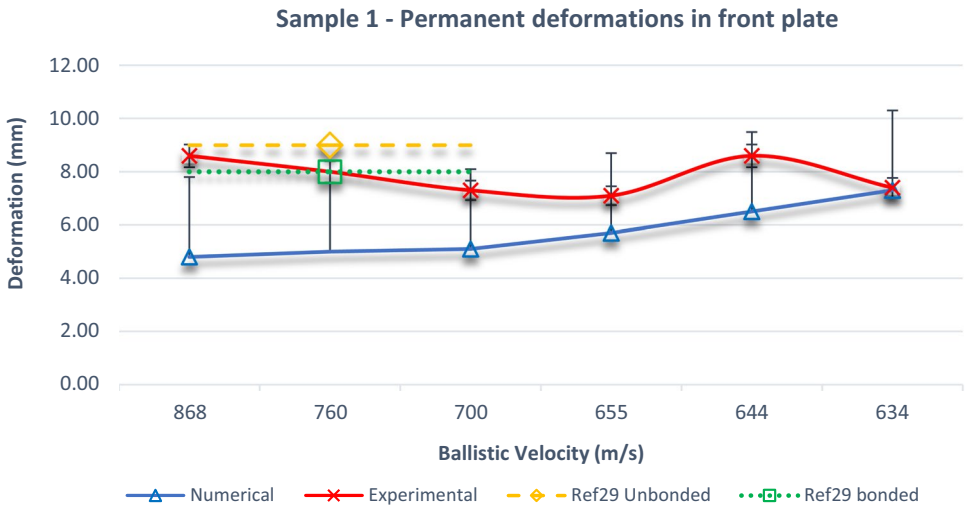

Fig. 15 Comparison of numerical analysis with experimental data for deformation results of the front plate

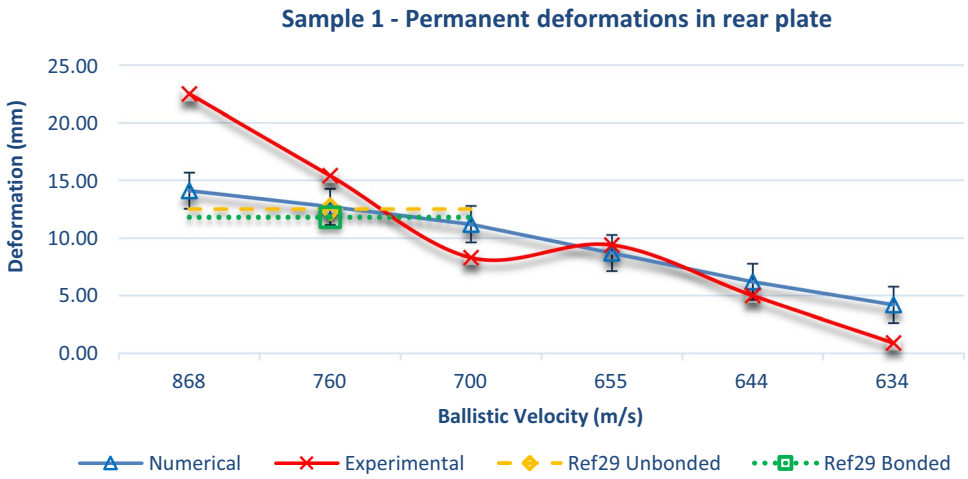

Fig. 16 Comparison of numerical analysis with experimental data for deformation results of the rear plate

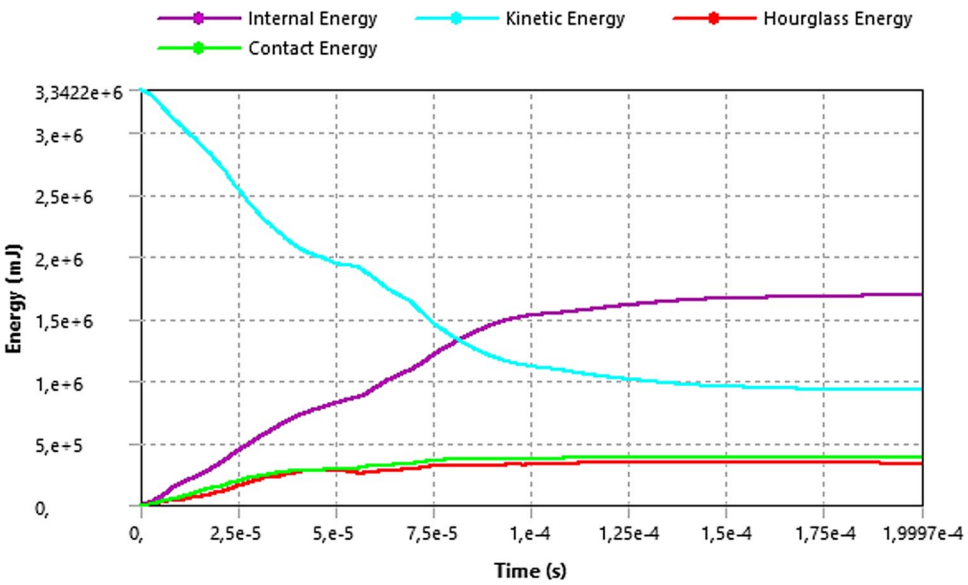

Fig. 17 System's energy distribution during ballistic upper limit analysis

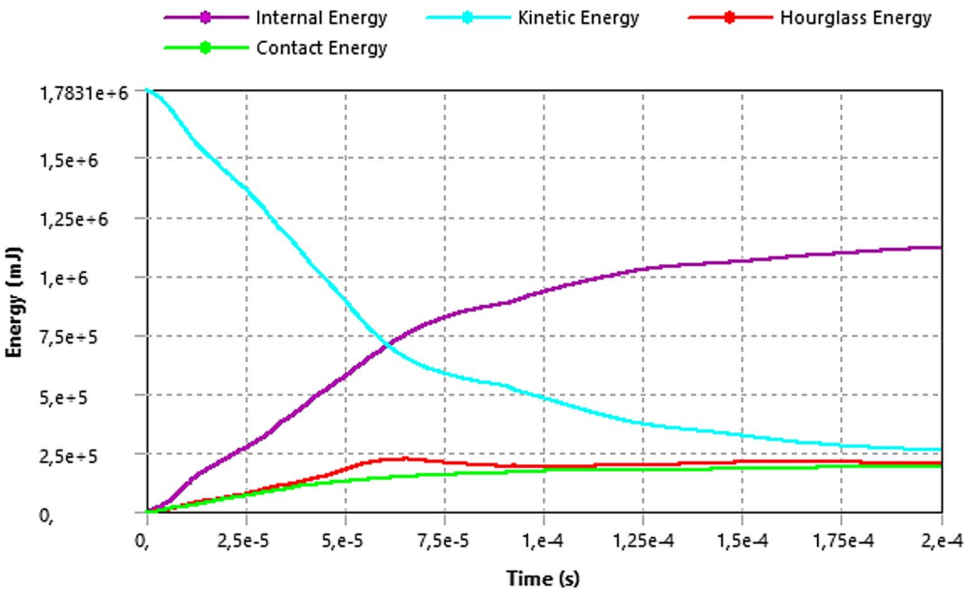

Fig. 18 System's energy distribution during ballistic lower limit analysis

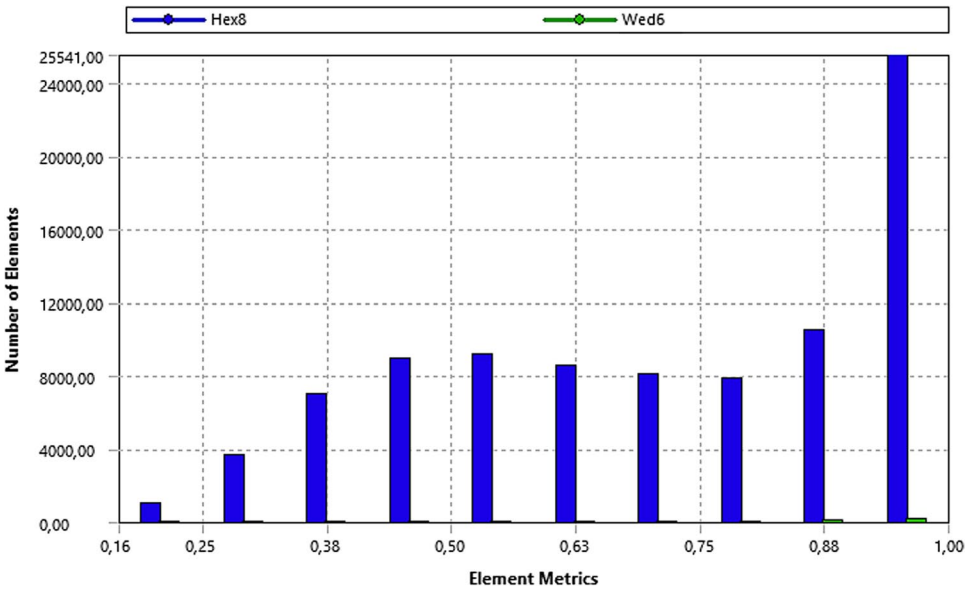

Fig. 19 Finite element quality diagram

- All samples 1, 2 and 3 did not cause any damage to the target when they were below 700 m/s bullet speed. However, at projectile velocities above 700 m/s (eg 768 and 866 m/s), the target is completely pierced.
- Shear bands can be observed because of returned tensile stress waves. The shear bands exposed that ballistic impact causes cyclic forcing in the sheets because of multiple reflections of the traction waves. In the rest of the fractured surface, ductile fracture type was observed throughout the thickness. Furthermore, mostly intergranular type fracture was observed from the fracture surface of the specimen.
- Researchers are advised to examine the similarity of the deformation behavior as well as the deformation values. Because only numerical comparison can be misleading due to small deviation range of values and particle losses.

Fig. 20 Finite elements model summary

Object Name	*Geometry*
State	Fully Defined
Definition	
Source	G:\Balistik\Analiz2_Conta_files\dp0\Geom-2\DM\Geom-2.agdb
Type	DesignModeler
Length Unit	Meters
Display Style	Body Color
Bounding Box	
Length X	74,4 mm
Length Y	300, mm
Length Z	215, mm
Properties	
Volume	1,0267e+006 mm³
Mass	7,3155e-003 t
Scale Factor Value	1,
Statistics	
Bodies	26
Active Bodies	26
Nodes	186961
Elements	90403
Mesh Metric	Element Quality
Min	0,16437
Max	0,99995
Average	0,70902
Standard Deviation	0,22525

Acknowledgements This project was supported by Research Fund of the Sakarya University of Applied Sciences. (Project Number: 2021-01-05-035). Thanks to Sakarya University of Applied Sciences due to financial support. We would also like to thank Otokar Company for providing the necessary support for ballistic experiments.

References

1. Kalay, Y. E. (2003). *Low velocity impact characterization of monolithic and laminated a 2024 plates by drop weight test*. MSc thesis, METU, Ankara, TR.
2. Backman, M. E., & Goldsmith, W. (1978). The mechanics of penetration of projectiles into targets. *International Journal of Engineering Science, 16*, 1–99.
3. Corbett, G. G., Reid, S. R., & Johnson, W. (1996). Impact loading of plates and shells by free-flying projectile. *International Journal of Impact Engineering, 18*(2), 141–230.
4. Hetherington, J., & Smith, P. (1994). *Blast and ballistic loading of structures*. CRC Press.
5. Shadbolt, P. J., Corran, R. S., & Ruiz, C. (1983). A comparison of plate perforation models in the sub-ordnance velocity range. *International Journal of Impact Engineering, 1*(1), 23–49.
6. Awerbuch, J. A., & Bodner, S. R. (1974). Analysis of the mechanics of perforation of projectiles in metallic plates. *International Journal of Solids and Structures, 10*, 671–684.
7. Langseth, M., & Larsen, P. K. (1992). The behavior of square steel plates subjected to a circular blunt ended load. *International Journal of Impact Engineering, 12*(4), 617–638.
8. Belytschko, T. (1996). On difficulty levels in nonlinear finite element analysis of solids. *Bulletin of the International Association for Computational Mechanics, 2*, 6–8.
9. Sundararajan, G. (1990). The energy absorbed during the oblique impact of a hard ball against ductile target materials. *International Journal of Impact Engineering, 9*(3), 343–358.
10. Goldsmith, W., & Finnegan, A. (1986). Normal and oblique impact of cylindro-conical and cylindrical projectiles on metallic plates. *International Journal of Impact Engineering, 4*, 83–90.
11. Guocai, W. (2005). The mechanical behavior of GLARE laminates for aircraft structures. *JOM Journal of the Minerals Metals and Materials Society, 57*, 72–79.
12. Ubeyli, M., Yıldırım, R. O., & Ogel, B. (2007). On the comparison of the ballistic performance of steel and laminated composite armors. *Materials & Design, 28*(4), 1257–1262.
13. Ubeyli, M., Yıldırım, R. O., & Ogel, B. (2008). Investigation on the ballistic behavior of Al2O3/Al2024 laminated composites. *Journal of Materials Processing Technology, 196*, 356–364.
14. Volt, A. (1996). Impact loading on fiber metal laminates. *International Journal of Impact Engineering, 18*(3), 291–307.
15. Ogorkiewicz, R. M. (1976). Composite armor. *Composites, 7*(2), 71–72.
16. Woodward, R. L. (1977). A rational basis for the selection or armor materials. *Journal of the Australian Institute of Metals, 22*, 167–170.
17. Manganello, J., & Abbott, K. H. (1972). Metallurgical factors affecting the ballistic behavior of steel targets. *Journal of Materials, JMLSA, 17*, 231–239.
18. Gupta, N. K., & Madhu, V. (1997). An experimental study of normal and oblique impact of hard-core projectile on single and layered plates. *International Journal of Impact Engineering, 19*, 395–414.
19. Medvedovski, E. (2010). Ballistic performance of armor ceramics: Influence of design and structure. Part 1. *Ceramics International, 36*, 2103–2115.
20. Medvedovski, E. (2010). Ballistic performance of armor ceramics: Influence of design and structure, part 2. *Ceramics International, 36*, 2117–2127.
21. Rabiei, A., & O'Neill, A. T. (2005). A study on processing of a composite metal foam via casting. *Materials Science and Engineering A, 404*, 159–164.

22. Neville, B. P., & Rabiei, A. (2008). Composite metal foams processed through powder metallurgy. *Materials and Design, 29*, 388–396.
23. Rabiei, A., & Garcia-Avila, M. (2013). Effect of various parameters on properties of composite steel foams under variety of loading rates. *Materials Science and Engineering A, 564*, 539–547.
24. Jena, P. K., Ramanjeneyulu, K., Siva Kumar, K., & Balakrishna Bhat, T. (2009). Ballistic studies on layered structures. *Materials and Design, 30*, 1922–1929.
25. Demir, T., Ubeyli, M., & Orhan Yıldırım, R. (2008). Investigation on the ballistic impact behavior of various alloys against 7.62 mm armor piercing projectile. *Materials and Design, 29*, 2009–2016.
26. Borvik, T., Langseth, M., Hopperstad, O. S., & Malo, K. A. (1999). Ballistic penetration of steel plates. *International Journal of Impact Engineering, 22*, 855–886.
27. Garcia-Avila, M., Portanova, M., & Rabiei, A. (2015). Ballistic performance of composite metal foams. *Composite Structures, 125*, 202–211.
28. TS EN 1522, Window, door, shutter, shutter-bullet resistance-properties and classification (**in Turkish**).
29. İbiş, Ö. M. *The effect of different number of layer and different joining techniques on ballistic performance in armor design*. Master's degree thesis, Graduate School of Natural and Applied Sciences, Sakarya University, Mechanical Engineering Department, 29.12.2021.
30. Lee, J. H., Park, S. J., Yang, J., Yeon, S. M., Hong, S., Son, Y., & Park, J. (2022). Crack guidance utilizing the orientation of additive manufactured lattice structure. *International Journal of Precision Engineering and Manufacturing, 23*, 797–805.
31. Ha, K., & Kim, J.-B. (2022). Collision analysis and residual longitudinal strength evaluation of a 5 MW spar floating offshore wind turbine impacted by a ship. *International Journal of Precision Engineering and Manufacturing-Green Technology, 9*, 841–858.
32. Crouch, I. G. (2017). *The science of armour materials* (pp. 55–115). Woodhead Publishing.
33. Flores-Johnson, E. A., Saleh, M., & Edwards, L. (2011). Ballistic performance of multilayered metallic plates impacted by a 7.62-mm APM2 projectile. *International Journal of Impact Engineering, 38*, 1022–1032.
34. Borvik, T., Dey, S., & Clausen, A. H. (2009). Perforation resistance of five different high strength steel plates subjected to small-arms projectiles. *International Journal of Impact Engineering, 36*, 948–964.
35. Johnson, G. R., & Cook, W. H. (1983). A constitutive model and data for metals subjected to large strains, high strain rates and high temperature. In *Proceedings 7th international symposium on ballistics, Lahey* (pp. 541–547).
36. Caliskan, M., Camcı, E., & Findik, F. (2022). Numerical and experimental investigation of the ballistic performance of the armor structure with in-layer deflector against bullets. *Latin American Journal of Solids and Structures, 19*(8), e470.
37. Garcia-Avila, M., Portanova, M., & Rabiei, A. (2013). Ballistic performance of a composite metal foam-ceramic armor system. In *Proceedings of Metfoam*.
38. Naik, N. K., Kumar, S., Ratnaveer, D., Joshi, M., & Akella, K. (2012). An energy-based model for ballistic impact analysis of ceramic-composite armors. *International Journal of Damage Mechanics, 22*, 145–187.
39. Backmann, M. E., & Goldsmith, W. (1978). The mechanics of penetration of projectiles into targets. *International Journal of Impact Engineering, 16*, 1–99.

Erdal Camcı works as a lecturer at Sakarya University of Applied Sciences Arifiye Vocational School. He graduated from Middle East Technical University, Mechanical Engineering Department. He completed his master's degree in Dumlupınar University, Institute of Sciences He worked as a research assistant at the same university for 3 years. He worked as a production engineer in the industrial sector for a while. He completed his doctoral study at Sakarya University in 2023. He took part in a project and has 3 articles. There is 1 patent application. His work is mainly on ballistic systems and their designs.

Mehmet Calışkan was born in 1970 in Zonguldak, Turkey. He graduated from Selçuk University, mechanical engineering department in 1995. He received a master's degree in Mechanical Engineering from Sakarya University in 1996. He received his doctorate degree in Mechanical Engineering from Sakarya University in 2002. The subject of his doctoral thesis is about armored vehicle design. He received the title of associate professor from the Turkish higher education institution in 2012. He received the title of professor from Sakarya University of Applied Sciences in 2023. He still continues his academic studies at this institution. As an author, he has published 11 indexed journal papers and 20 conference papers in international and national conferences. He has also 1 book and 1 book chapter published in his scientific area. Also, he is actively involved as reviewer for leading journals for several SCI journals.

İlyas Berkay Tural serves as a ballistic protection and firing power tests specialist engineer at Otokar Otomotiv ve Savunma Sanayi A.Ş Turkey. He graduated from Yeditepe University Mechanical Engineering Department in 2018. He participated in many scientific conferences and he has 1 patent.

Özgecan Ergü was born in 1979. She graduated from Gazi University, Department of Chemical Engineering in 2003. She received her master's degree in Chemical Engineering from Gazi University in 2006. She received her doctorate degree in chemical engineering from Ataturk University in 2011. She currently works at the Turkish Ministry of National Defense.

Fehim Findik serves as a Professor at Department of Metallurgy and Materials Engineering, Sakarya University of Applied Sciences, Turkey. He received his MSc in mechanical engineering from Istanbul Technical University and Ph.D. degree in materials engineering from Imperial College of London University, UK, in 1992. His main scientific interests include materials science, selection of materials and manufacturing, especially composite processing, light & super alloys, biomaterials, implants & stents, powder metallurgy applications and mechanical behavior of materials. He teaches courses at both undergraduate and post-graduate levels in the above mentioned areas. He has done post-doctoral studies in UK, Canada, and USA. He participated in many scientific conferences. As an author, he has 3 patents and published 100 SCI-indexed journal papers and 80 conference papers in international conferences as well as more than 3500 citations in SCI journals. He has also 5 books and 5 book chapters published in his scientific area. Also, he is actively involved as reviewer for leading journals including Materials and Design, Biomaterials, Powder Metallurgy, Alloys and Compounds as well as managing in the editorial board for several SCI journals.